

Minimum entropy deconvolution and simplicity: A noniterative algorithm

Carlos A. Cabrelli*

ABSTRACT

Minimum entropy deconvolution (MED) is a technique developed by Wiggins (1978) with the purpose of separating the components of a signal, as the convolution model of a smooth wavelet with a series of impulses.

The advantage of this method, as compared with traditional methods, is that it obviates strong hypotheses over the components, which require only the simplicity of the output. The degree of simplicity is measured with the Varimax norm for factor analysis. An iterative algorithm for computation of the filter is derived from this norm, having as an outstanding characteristic its stability in presence of noise.

Geometrical analysis of the Varimax norm suggests the definition of a new criterion for simplicity: the D norm. In case of multiple inputs, the D norm is obtained through modification of the kurtosis norm.

One of the most outstanding characteristics of the new criterion, by comparison with the Varimax norm, is that a noniterative algorithm for computation of the deconvolution filter can be derived from the D norm. This is significant because the standard MED algorithm frequently requires in each iteration the inversion of an autocorrelation matrix whose order is the length of the

filter, while the new algorithm derived from the D norm requires the inversion of a single matrix.

On the other hand, results of numerical tests, performed jointly with Graciela A. Canziani¹, show that the new algorithm produces outputs of greater simplicity than those produced by the traditional MED algorithm. These considerations imply that the D criterion yields a new computational method for minimum entropy deconvolution.

A section of numerical examples is included, where the results of an extensive simulation study with synthetic data are analyzed. The numerical computations show in all cases a remarkable improvement resulting from use of the D norm. The properties of stability in the presence of noise are preserved as shown in the examples.

In the case of a single input, the relation between the D norm and the spiking filter is analyzed (Appendix B).

¹Instituto Argentino de Matemática, Consejo Nacional de Investigaciones Científicas y Técnicas, Viamonte 1636, 1055 Buenos Aires, and Departamento de Matemática, Universidad de Buenos Aires, Pabellón I, Ciudad Universitaria, 1428 Buenos Aires, Argentina.

INTRODUCTION

The minimum entropy deconvolution (MED) technique represents a new and interesting approach to the problem of deconvolution. First proposed in Wiggins (1978), the technique was later improved by Ooe and Ulrych (1979) who incorporated an exponential transformation into the original algorithm. Recently, the technique was again considered in papers by Oldenburg et al. (1981) and Ulrych and Walker (1982).

Deconvolution, a standard topic in signal processing, is also used in astronomy, seismic signals, radar, and image processing. A wide range of physical processes can be described by a system where a source signal is perturbed in order to produce an observable output (Figure 1).

The system is usually represented by an operator S which acts on the source signal w by means of a convolution. Moreover, if an additive noise component η is introduced, the model is represented by

$$y = S * w + \eta$$

where $*$ denotes convolution.

The deconvolution process involves separation of the components of convolution in the observed signal y . Satisfactory results were obtained when one component was known (Clayton and Ulrych, 1977). However, when only the observed signals y are known, the problem becomes much more difficult. Here, uniqueness is lost and strong hypotheses over the components must be made. Validity of the model will then depend

Manuscript received by the Editor January 23rd, 1984; revised manuscript received September 4, 1984.

*Departamento de Matemática Facultad de Ciencias Exactas y Naturales Universidad de Buenos Aires, Pabellon I, Ciudad Universitaria 1428 Buenos Aires, Argentina.

© 1985 Society of Exploration Geophysicists. All rights reserved.

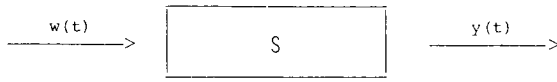


FIG. 1. The system is usually represented by an operator S which acts on the source signal w by means of a convolution, producing an observable output y .

upon the extent to which the physical process can be adjusted to these hypotheses.

Several solutions have been tried with success, although strong restrictions over the components had to be made. With predictive deconvolution (Robinson and Treitel, 1980), for example, some good results are obtained under the assumption of minimum phase for the source signal and white noise for the reflectivity function. An excellent review of these techniques is presented in Lines and Ulrych (1977).

The advantage of the MED lies in elimination of these hypothesis, under only the assumption of "simplicity" for the desired signal, thus introducing a concept used in factor analysis.

In this paper, the criterion for simplicity used by Wiggins (1978) is analyzed, and it is shown that certain geometrical, rather than statistical, considerations suggest another criterion for simplicity, which, together with the kurtosis norm used by Ooe and Ulrych (1979), leads into a noniterative algorithm for MED.

THEORETICAL CONSIDERATIONS

Consider N observed signals x_1, \dots, x_N . For each i ($i = 1, \dots, N$), let x_i be represented by

$$x_i = w * q_i + \eta_i.$$

That is, each signal is considered as the convolution of a source signal w (same for all x_i) with a disturbance signal q_i and contaminated with an additive noise η_i .

Now suppose that each signal x_i is convolved with the same filter f in order to obtain an output

$$y_i = f * x_i = (f * w) * q_i + f * \eta_i \quad (i = 1, \dots, N).$$

If the q_i 's ($i = 1, \dots, N$) are the desired signals, the filter f should be such that $(f * w) * q_i$ approximates q_i , which could be obtained if f represents an inverse of w . At the same time it should suppress noise, that is, elimination of terms $f * \eta_i$ ($i = 1, \dots, N$).

The MED method assumes that the output y_i resulting from the application of the filter f on x_i is of a "simple" structure.

The concept of "simplicity" or parsimony for a data matrix $\mathbf{A} = (a_{ij})$ is one of the main points of factor analysis in multivariate analysis. Roughly speaking, a simple structure for a matrix \mathbf{A} means that almost all its coefficients are nearly zero, while a few of them take arbitrary values and location.

More than twenty years elapsed before a satisfactory way was found to set this concept in precise mathematical terms (Carroll, 1953). The solution consisted in the definition of a "norm" that could measure the degree of simplicity of a matrix. Later a diversity of norms or simplicity criteria were considered

(Harman, 1960). The problem of choosing the matrix with greatest simplicity from an infinite set of matrices which vary according to certain parameters now turns into the maximization or the minimization of a norm over the set mentioned above. The chosen norm should be such that a satisfactory algorithm, from the computational point of view, could be derived from it.

Wiggins (1978) proposed the varimax norm or criterion defined for a matrix $\mathbf{A} = (a_{ij})$ by

$$V(\mathbf{A}) = \sum_i V_i(\mathbf{A}),$$

where

$$V_i(\mathbf{A}) = \sum_j \frac{a_{ij}^4}{(\sum_k a_{ik}^2)^2}.$$

In statistical terms, $V_i(\mathbf{A})$ represents the variance of the squares of the entries of each normalized row of \mathbf{A} .

The varimax criterion is then applied to the outputs $\mathbf{Y} = (y_{ij})$ in order to maximize $V(\mathbf{Y})$ over all filters $\mathbf{f} = (f_1, \dots, f_\ell)$ of fixed length ℓ . Differentiating $V(\mathbf{Y})$ with respect to the filter coefficients f_k and equating to zero, a set of equations is obtained which can be rewritten in matrix form as

$$\mathbf{R}(\mathbf{f}) \cdot \mathbf{f} = \mathbf{g}(\mathbf{f}),$$

where $\mathbf{R} = \mathbf{R}(\mathbf{f})$ is a Toeplitz matrix and $\mathbf{g} = \mathbf{g}(\mathbf{f})$ a column vector whose coefficients depend upon \mathbf{f} .

Choosing an initial filter $\mathbf{f}^0 = (0, \dots, 0, 1, 0, \dots, 0)$, an iterative algorithm can be generated by taking

$$\mathbf{f}^{n+1} = \{\mathbf{R}(\mathbf{f}^n)\}^{-1} \mathbf{g}(\mathbf{f}^n),$$

which leads to a satisfactory solution.

GEOMETRICAL INTERPRETATION OF THE VARIMAX NORM

In the case of a single sample input, let $\mathbf{y} \in \mathbb{R}^m$, $\mathbf{y} \neq 0$. Consider the Varimax norm

$$V(\mathbf{y}) = \sum_i y_i^4 / (\sum_k y_k^2)^2. \quad (1)$$

If the Euclidian norm of \mathbf{y} is noted by

$$\|\mathbf{y}\| = (\sum_k y_k^2)^{1/2},$$

then (1) becomes

$$V(\mathbf{y}) = \sum_i \left(\frac{y_i}{\|\mathbf{y}\|} \right)^4.$$

The norm V is homogeneous,

$$V(\lambda \mathbf{y}) = V(\mathbf{y}) \quad (2)$$

for $\lambda \in \mathbb{R}$, $\lambda \neq 0$. Besides, V can be factorized as a composition of two transformations

$$(y_1, \dots, y_m) \xrightarrow{T_1} [(y_1/\|\mathbf{y}\|)^2, \dots, (y_m/\|\mathbf{y}\|)^2],$$

and

$$(y_1, \dots, y_m) \xrightarrow{T_2} \sum_i y_i^2 = \|\mathbf{y}\|^2.$$

This means that

$$V(y) = T_2 [T_1(y)].$$

Let us now analyze the effect of T_1 on a vector y . First consider

$$H = \{(x_1, \dots, x_m) \in \mathbb{R}^m \mid \sum_i x_i = 1, x_i \geq 0, i = 1, \dots, m\}.$$

The transformation T_1 takes a vector $y \in \mathbb{R}^m$ to a vector of the region H , since

$$\sum_i (y_i / \|y\|)^2 = \|y\|^{-2} \sum_i y_i^2 = \|y\|^2 / \|y\|^2 = 1$$

and $(y_i / \|y\|)^2 \geq 0$ for all i . Moreover, any vector in the direction of y will have the same image as y .

In Figure 2a, H is represented in the case $m = 3$ and in Figure 2b it is shown how T_1 transforms the vectors y_1 and y_2 . Note, that in Figure 2b H is the segment joining e_1 and e_2 , and $m = 2$. This transformation slightly modifies the angles between the vector and the coordinate axes because the coordinates are squared.

The transformation T_2 , defined over H , reaches its minimum at the barycenter $B = (m^{-1}, \dots, m^{-1})$ and its maxima at e_1, \dots, e_m , the vertices of H (with m being the dimension of the space \mathbb{R}^m), and increases as the distance from y to point B increases. This means that T_2 measures the withdrawal of a vector y from B or the equivalent, its proximity to the set of vertices. Therefore, the simplicity of a vector following the varimax criterion increases with its proximity to any of the vertices.

Considering the homogeneity of V , the simplicity of any nonzero vector of \mathbb{R}^m is given as a function of the angles formed by the line defined by the vector and the coordinate axes: the closer the line is to one of the axes, the higher the simplicity is (and the higher the modulus of the corresponding cosines).

Also note that, for $y \in \mathbb{R}^m, y \neq 0, V(y)$ lies between the boundaries

$$m^{-1} \leq V(y) \leq 1.$$

Figure 3, illustrates the contour lines of transformation T_2 defined on H , for $m = 3$.

VARIMAX NORM AND DECONVOLUTION

Let x, f , and y be vectors of length n, ℓ , and $m = n + \ell - 1$, respectively, and suppose that

$$y = x * f,$$

i.e.,

$$y_k = \sum_s f_s x_{k+1-s} \quad k = 1, \dots, m, \tag{3}$$

where $x_i = 0$ if $i \notin \{1, \dots, n\}$.

Written in matrix form equation (3) becomes

$$(y_1, \dots, y_m) = (f_1, \dots, f_\ell) \begin{bmatrix} x_1 & x_2 & \dots & x_n & 0 & \dots & 0 \\ 0 & x_1 & \dots & \dots & \dots & \dots & 0 \\ \dots & \dots & \dots & \dots & \dots & \dots & \dots \\ 0 & \dots & 0 & x_1 & x_2 & \dots & x_n \end{bmatrix} \tag{4}$$

Therefore, $y = f \cdot X$, where X is a $\ell \times m$ matrix. If v_k is the k th row of matrix X , we can write y as a linear combination of vectors v_k , where the coefficients are coordinates of the filter f :

$$y = \sum_k f_k v_k.$$

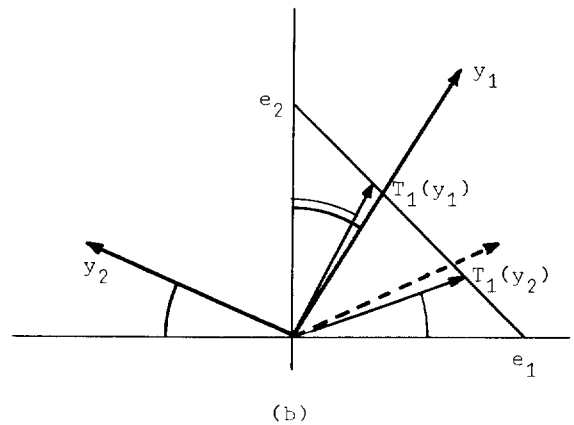
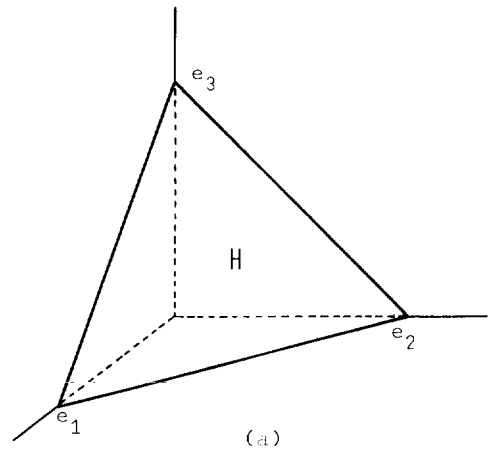


FIG. 2. (a) The region H for $m = 3$. (b) Effect of the transformation T_1 on 2-D vectors.

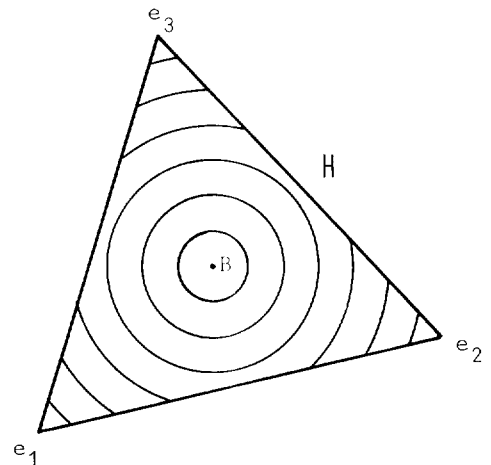


FIG. 3. Contour lines for transformation T_2 .

The vectors v_k are linearly independent (see Appendix A), hence they span an ℓ -dimensional linear subspace W of \mathbb{R}^m .

Each nonzero filter f generates a vector y , whose simplicity can be measured with norm V

$$f \mapsto y \mapsto V(y)$$

$$\mathbb{R}^\ell - \{0\} \mapsto W \mapsto \mathbb{R}.$$

EQUIVALENCE OF CRITERIA

A criterion of simplicity for a set of vectors $A \subset \mathbb{R}^n$ can be defined as a function

$$C : A \rightarrow \mathbb{R}.$$

Two criteria C_1 and C_2 defined over a set A are equivalent if

$$\text{for all } x, y \in A \quad C_1(x) \leq C_1(y) \Leftrightarrow C_2(x) \leq C_2(y),$$

or if

$$\text{for all } x, y \in A \quad C_1(x) \leq C_1(y) \Leftrightarrow C_2(x) \geq C_2(y).$$

Clearly, two equivalent criteria should reach their extrema at the same vectors; therefore the selection of one or another will depend upon the algorithmic complexity derived from them.

If $C_1 = aC_2 + b$, $a \neq 0$, $a, b \in \mathbb{R}$, then C_1 and C_2 are equivalent. For example, the varimax norm and the norm $\|T_1(y) - B\|^2$, where B is the barycenter of H , are equivalent since

$$\begin{aligned} \|T_1(y) - B\|^2 &= \sum_i \{(y_i/\|y\|)^2 - m^{-1}\}^2 \\ &= \sum_i (y_i/\|y\|)^4 - 2m^{-1} \sum_i (y_i/\|y\|)^2 + \sum_i m^{-2} \\ &= V(y) - m^{-1}. \end{aligned}$$

Subsequently, I define another criterion of simplicity from which a noniterative algorithm can be derived and which has given satisfactory results.

THE D NORM

Analysis of the Varimax norm indicates the need to measure the simplicity of a vector y as a function of the distance from y to the points e_1, \dots, e_{2m} where

$$e_k = (0, \dots, 1_k, \dots, 0) \quad k = 1, \dots, m,$$

and

$$e_{m+k} = (0, \dots, -1_k, \dots, 0) \quad k = 1, \dots, m.$$

Now define

$$D_1(y) = \min_{1 \leq i \leq 2m} \|(y/\|y\|) - e_i\|^2$$

where the normalization of y is intended to preserve homogeneity [equation (2)].

We have

$$\|(y/\|y\|) - e_k\|^2 = 2 - 2(y_k/\|y\|), \quad k = 1, \dots, m$$

and

$$\|(y/\|y\|) - e_{m+k}\|^2 = 2 + 2(y_k/\|y\|), \quad k = 1, \dots, m.$$

Hence

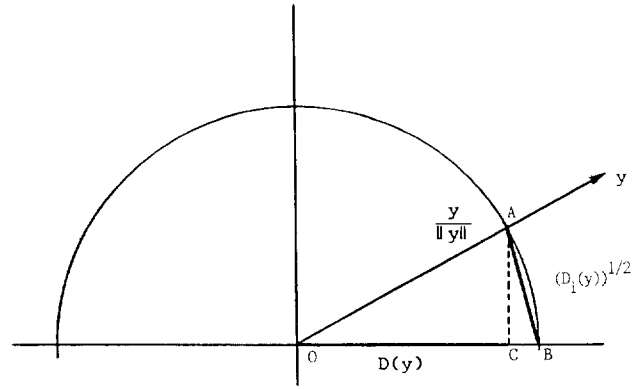


FIG. 4. Norms D and D_1 of a given vector $y(m = 2)$.

$$\min_{1 \leq i \leq 2m} \|(y/\|y\|) - e_i\|^2 = 2\{1 - \max_{1 \leq k \leq m} (|y_k|/\|y\|)\}.$$

Therefore, by defining

$$D(y) = \max_{1 \leq k \leq m} |y_k|/\|y\|$$

then

$$D_1(y) = 2 - 2D(y).$$

Consequently, D_1 and D are equivalent criteria, in this sense.

In Figure 4, the length of the segment AB represents the distance between $y/\|y\|$ and e_1 —this is $[D_1(y)]^{1/2}$ —and the length of OB is $D(y)$.

Figure 5 presents a graph of the behavior of norms D and V by changing the filter in three different outputs. In all cases $x = (x_1, x_2)$ (an input trace of length 2) has been convolved with a filter of the same length $f = (f_1, f_2)$.

Since the norms have the property of homogeneity, it is sufficient to consider

$$f_\alpha = (\cos \alpha, \sin \alpha)$$

for each $\alpha \in (0, 2\pi)$. The curves represent $V(y_\alpha)$ and $D(y_\alpha)$, where

$$y_\alpha = x * f_\alpha.$$

THE D NORM AND DECONVOLUTION

When using the D criterion to solve the problem of deconvolution in the case of a single sample input, maximize $D(y)$, $y = f * x$ over all nonzero filters $f = (f_1, \dots, f_\ell)$ of fixed length ℓ . The result is

$$\begin{aligned} \sup_{f \in \mathbb{R}^\ell} D(y) &= \sup_{f \in \mathbb{R}^\ell} \{ \max_i (|y_i|/\|y\|) \} \\ &= \max_i \{ \sup_{f \in \mathbb{R}^\ell} (|y_i|/\|y\|) \}. \end{aligned} \tag{5}$$

Since f is a maximum of $|y_i|/\|y\|$ [if, and only if, f is an extremal point (maximum or minimum) of $y_i/\|y\|$], it is then equivalent in equation (5) to find first the extrema of $y_i/\|y\|$ for each i and then the maximum over i .

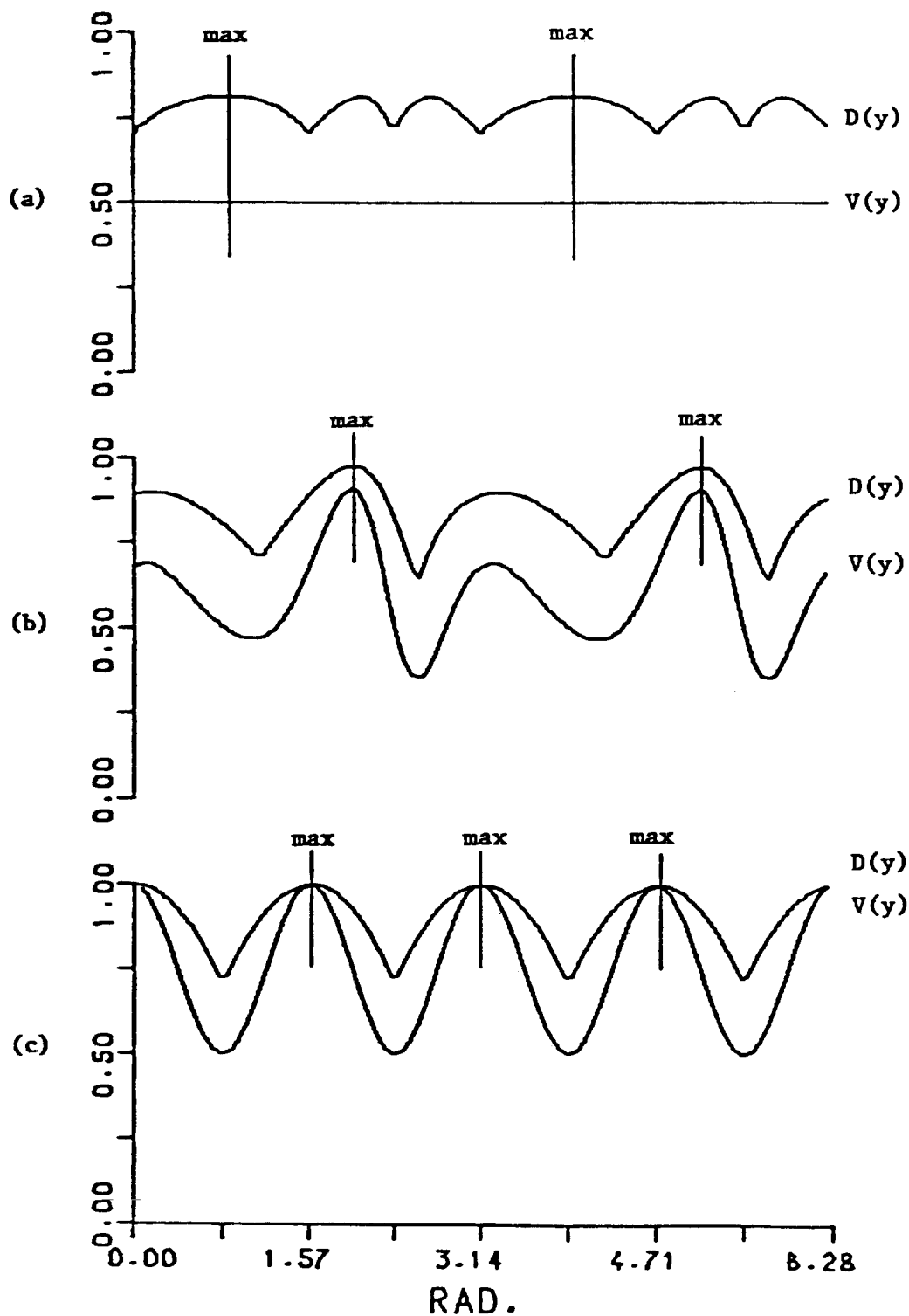


FIG. 5. Plots of the norms $D(y)$ and $V(y)$ for vectors $y = f * x$, where $f = (\cos \alpha, \sin \alpha)$, $\alpha \in [0, 2\pi]$, and $x \in \mathbb{R}^2$ such that (a) $x = (1, 1)$; (b) $x = (-1, -2)$, and (c) $x = (100, 1)$.

Hence the extrema for each fixed i are found by differentiating with respect to the coefficients f_k of the filter and equating to zero:

$$\frac{\partial}{\partial f_k} (y_i / \|\mathbf{y}\|) = 0; \quad k = 1, \dots, \ell.$$

From

$$\|\mathbf{y}\| = \left(\sum_j y_j^2 \right)^{1/2}$$

and

$$y_i = \sum_s f_s x_{i-s+1}$$

it follows that

$$\frac{\partial y_i}{\partial f_k} = x_{i-k+1}$$

and

$$\frac{\partial \|\mathbf{y}\|}{\partial f_k} = \|\mathbf{y}\|^{-1} \sum_j y_j \frac{\partial y_j}{\partial f_k} = \|\mathbf{y}\|^{-1} \sum_j y_j x_{j-k+1}.$$

Therefore

$$\begin{aligned} \frac{\partial}{\partial f_k} (y_i / \|\mathbf{y}\|) &= \|\mathbf{y}\|^{-2} \{x_{i-k+1} \|\mathbf{y}\| - \|\mathbf{y}\|^{-1} (\sum_j y_j x_{j-k+1}) y_i\} \\ &= \|\mathbf{y}\|^{-1} \{x_{i-k+1} - y_i \|\mathbf{y}\|^{-2} \\ &\quad \times (\sum_j \sum_s f_s x_{j-s+1} x_{j-k+1})\}. \end{aligned}$$

Equating to zero, gives,

$$(y_i / \|\mathbf{y}\|^2) \sum_s f_s \sum_j (x_{j-s+1} x_{j-k+1}) = x_{i-k+1}.$$

Let

$$r_{s-k} = \sum_j x_{j-s+1} x_{j-k+1}.$$

Then write

$$(y_i / \|\mathbf{y}\|^2) \sum_s f_s r_{s-k} = x_{i-k+1} \quad k = 1, \dots, \ell,$$

which can in turn be written in matrix form as

$$(y_i / \|\mathbf{y}\|^2) \mathbf{R} \cdot \mathbf{f} = \mathbf{x}^i$$

where

$$\mathbf{R} = \begin{bmatrix} r_0 & r_1 & \cdots & r_{\ell-1} \\ r_1 & r_0 & & \cdot \\ \cdot & \cdot & & \cdot \\ \cdot & \cdot & & r_1 \\ r_{\ell-1} & & & r_0 \end{bmatrix}$$

is the matrix of autocorrelations of the input sample and \mathbf{x}^i is the vector

$$\mathbf{x}^i = [x_i, x_{i-1}, \dots, x_{i-(\ell-1)}]$$

with $x_k = 0$ if $k \notin \{1, \dots, m\}$.

MULTIPLE SAMPLE INPUT

In the case of multiple inputs, the varimax norm maximizes

the sum of the varimax of each input. This generalization for norm D leads to a nonefficient algorithm from the computational point of view.

Nevertheless, the D norm can be extended to the case of multiple inputs, giving a noniterative algorithm of easy computation, by exploiting the idea implicit in the kurtosis norm.

Consider N signals \mathbf{y}_i ($i = 1, \dots, N$) of length m , where

$$y_{ij} = \sum_k f_k x_{i,j-k+1} \quad j = 1, \dots, m.$$

The kurtosis norm of matrix $\mathbf{Y} = (y_{ij})$ is defined by

$$K(\mathbf{Y}) = \sum_i \sum_j (y_{ij} / \|\mathbf{Y}\|)^4$$

where

$$\|\mathbf{Y}\| = \left(\sum_{i,j} y_{ij}^2 \right)^{1/2}$$

(Ooe and Ulrych, 1979).

This means that $K(\mathbf{Y})$ is the varimax norm applied to an Nm -dimensional vector whose coordinates are obtained by placing the rows of matrix \mathbf{Y} one after the other, as

$$(y_{11}, \dots, y_{1m}, y_{21}, \dots, y_{2m}, \dots, y_{N1}, \dots, y_{Nm}).$$

The D norm applied to this vector yields

$$D(\mathbf{Y}) = \max_{i,j} (|y_{ij}| / \|\mathbf{Y}\|).$$

The aim is then to compute

$$\max_{i,j} \left\{ \sup_{f \in \mathbb{R}^\ell} (|y_{ij}| / \|\mathbf{Y}\|) \right\}$$

for all nonzero filters of fixed length ℓ .

NORMAL EQUATIONS FOR THE D NORM

Consider the matrix $\mathbf{Y} = (y_{ij})$, where

$$y_{ij} = \sum_k f_k x_{i,j-k+1} \quad \begin{matrix} i = 1, \dots, N \\ j = 1, \dots, m \end{matrix}$$

From this and

$$\|\mathbf{Y}\| = \left(\sum_{r,t} y_{rt}^2 \right)^{1/2},$$

it follows that

$$\frac{\partial y_{ij}}{\partial f_s} = x_{i,j-s+1},$$

and

$$\begin{aligned} \frac{\partial \|\mathbf{Y}\|}{\partial f_s} &= (2\|\mathbf{Y}\|)^{-1} \sum_{r,t} 2y_{rt} \frac{\partial y_{rt}}{\partial f_s} \\ &= \|\mathbf{Y}\|^{-1} \sum_{r,t} y_{rt} x_{r,t-s+1} \\ &= \|\mathbf{Y}\|^{-1} \sum_{r,t} \sum_k f_k x_{r,t-k+1} x_{r,t-s+1} \\ &= \|\mathbf{Y}\|^{-1} \sum_k f_k \sum_r \left(\sum_t x_{r,t-k+1} x_{r,t-s+1} \right). \end{aligned}$$

If

$$\Gamma_{k-s} = \sum_t x_{r,t-k+1} x_{r,t-s+1},$$

the autocorrelation of x_r in $(k-s)$, then

$$\begin{aligned}\frac{\partial \|\mathbf{Y}\|}{\partial f_s} &= \|\mathbf{Y}\|^{-1} \sum_k f_k \sum_r \Gamma_{k-s}^r \\ &= \|\mathbf{Y}\|^{-1} \sum_k f_k \Gamma_{k-s}, \quad \text{if } \Gamma_i = \sum_j \Gamma_j^i.\end{aligned}$$

Finally, this gives

$$\begin{aligned}\frac{\partial}{\partial f_s} (y_{ij}/\|\mathbf{Y}\|) &= \|\mathbf{Y}\|^{-2} \left(\frac{\partial y_{ij}}{\partial f_s} \|\mathbf{Y}\| - \frac{\partial \|\mathbf{Y}\|}{\partial f_s} y_{ij} \right) \\ &= \|\mathbf{Y}\|^{-2} (x_{i, j-s+1} \|\mathbf{Y}\| - \|\mathbf{Y}\|^{-1} \\ &\quad \times \sum_k f_k \Gamma_{k-s} y_{ij}).\end{aligned}$$

Equating this to zero in order to obtain the extrema, then

$$y_{ij} \|\mathbf{Y}\|^{-2} \sum_k f_k \Gamma_{k-s} = x_{i, j-s+1} \quad s = 1, \dots, \ell,$$

which can be expressed in matrix form by writing

$$(y_{ij}/\|\mathbf{Y}\|^2) \mathbf{R} \cdot \mathbf{f} = \mathbf{x}^{ij} \quad (6)$$

where

$$\mathbf{R} = \sum_i \mathbf{R}^i,$$

with \mathbf{R}^i the matrix of autocorrelations of the i th sample input, and $\mathbf{x}^{ij} = [x_{ij}, x_{i, j-1}, \dots, x_{i, j-(\ell-1)}]$, with $x_{ik} = 0$ if $k \notin \{1, \dots, m\}$. From equation (6)

$$(y_{ij}/\|\mathbf{Y}\|^2) \cdot \mathbf{f} = \mathbf{R}^{-1} \mathbf{x}^{ij}. \quad (7)$$

If \mathbf{f}° is a solution of equation (7), then $\lambda \mathbf{f}^\circ$ is also a solution of this equation, since

$$\frac{y_{ij}(\lambda \mathbf{f}^\circ)}{\|\mathbf{Y}(\lambda \mathbf{f}^\circ)\|^2} \lambda \mathbf{f}^\circ = \frac{\lambda y_{ij}(\mathbf{f}^\circ)}{\lambda^2 \|\mathbf{Y}(\mathbf{f}^\circ)\|^2} \lambda \mathbf{f}^\circ = \frac{y_{ij}}{\|\mathbf{Y}\|^2} \mathbf{f}^\circ$$

where $\mathbf{Y}(\mathbf{f})$ denotes the output obtained by applying the filter \mathbf{f} and $y_{ij}(\mathbf{f})$ its ij -coordinate.

In particular, if \mathbf{f}° satisfies equation (7), then \mathbf{f}° is a multiple of vector $\mathbf{R}^{-1} \mathbf{x}^{ij}$. This means that $\mathbf{f} = \mathbf{R}^{-1} \mathbf{x}^{ij}$ is a solution. If

$$\mathbf{f}^{ij} = \mathbf{R}^{-1} \mathbf{x}^{ij},$$

the algorithm terminates by computing

$$\max_{i, j} (|y_{ij}^{(ij)}| / \|\mathbf{Y}^{(ij)}\|),$$

where $\mathbf{Y}^{(ij)}$ is the output obtained by applying the filter \mathbf{f}^{ij} .

NUMERICAL EXAMPLES

(In collaboration with G. A. Canziani¹)

Computational procedure and implementation

I call MED the algorithm obtained by Wiggins (1978) from the Varimax norm, and f_v the corresponding filter. Correspondingly MEDD and f_D will, respectively, denote the algorithm and the filter obtained from the D norm.

Because MED and MEDD entail autocorrelation matrices, which are Toeplitz forms, we use the Levinson recursion in their inversion.

The MEDD algorithm is noniterative. One of its advantages is that it requires computation and inversion of just one autocorrelation matrix whose order is equal to the chosen filter length.

All the tested examples indicate that the optimum filter length for the MEDD algorithm is smaller than for the MED algorithm.

Fast convolution and crosscorrelation algorithms using fast Fourier transforms (FFT), essential to digital signal processing, have been incorporated in both MED and MEDD algorithms to improve efficiency.

Convergence

Note that initializing the filter in the MED algorithm to $\mathbf{f}_v^0 = (0, \dots, 1, \dots, 0)^t$ the value of the varimax norm of the output $\mathbf{y}^{(n)} = \mathbf{f}_v^{(n)} * \mathbf{x}$, obtained from the n th iteration, grows significantly during the first N iterations (N depending on the input characteristics and the chosen filter length) until it becomes steady. This limits the MED algorithm since thereafter it is not possible to make any improvement in the simplicity of the input.

In the examples considered the Varimax norm of the MEDD output achieves values exceeding the maximum values reached by the Varimax norm of the MED output, when the chosen filter lengths used in both procedures are optimal. This can be written

$$V(\mathbf{y}_{rD}) \geq V(\mathbf{y}_{rV}),$$

where

$$\mathbf{y}_{rD} = \mathbf{x} * \mathbf{f}_D, \quad (8)$$

and

$$\mathbf{y}_{rV} = \mathbf{x} * \mathbf{f}_V.$$

This means that the MEDD algorithm produces an output of greater simplicity, when simplicity is measured through the Varimax norm.

However, outputs obtained by means of both methods maintain the same relation of order, relative to the D norm (see Table 1). That is,

$$D(\mathbf{y}_{rD}) \geq D(\mathbf{y}_{rV}).$$

A larger varimax or D norm value is not a measure of success if the original reflectivity series is not reproduced. However, when the reflectivity was reproduced successfully, the inequality (8) suggests a better signal-to-noise ratio for the MEDD output which is definitely desirable.

Note that the inequality (8) has not been confirmed in general yet, but it holds for all the considered examples.

THE EXAMPLES

An extensive simulation study was carried out with synthetic data. First a comparative study of both methods was made, and subsequently the MEDD's efficiency was tested in the case of data contaminated with white noise.

Six examples are used to make evident the valuable charac-

¹Instituto Argentino de Matemática, Consejo Nacional de Investigaciones Científicas y Técnicas, Viamonte 1636, 1055 Buenos Aires, and Departamento de Matemática, Universidad de Buenos Aires, Pabellón I, Ciudad Universitaria, 1428 Buenos Aires, Argentina.

teristics of the new algorithm. Three of them show results obtained through both methods with multiple trace inputs, using different types of source wavelets. For each example I present a graph showing the convergence of the Varimax norm of the MED outputs, as compared with that of the MEDD outputs. The last three examples refer to the behavior of the MEDD algorithm when different percentages of noise are added to the inputs.

In the examples where white noise was added to the input traces, the percentages of noise represent the largest noise amplitude as percentage of the largest signal amplitude.

In all cases the source wavelet was recovered by inversion of the filter. This inversion has been done by taking the filter as input of the MEDD algorithm and choosing the length of the source wavelet as that of the inverted filter.

For each example, the MEDD filter has been convolved with the source wavelet, resulting in a function which approximates the delta function. Adjustment of this approximation shows how good an approximation to the inverse of the source wavelet the filter is.

It is worth noting that the polarity or delay of the output spikes does not affect the maximization. These should be adjusted by comparing output with input. Generally, if the negative lobes are larger in average than the positive, the polarity will appear reversed.

In order to make the reflectors $q(t)$ occur at each time sample, in all the examples 1 percent white noise was added to $q(t)$.

Examples 1 to 3. Model $x = w * q$

Example 1.—The aim of this example is to study the behavior of both methods in the case where the source wavelet is a damped wavelet (96 units long). Two four-impulse randomly generated spike series were used. Figure 6a shows $w(t)$, $q(t)$, and the convolved input trace $x(t) = w(t) * q(t)$ used in both MED and MEDD algorithms.

Usually the correct value of the filter length cannot be foreseen straightforwardly, and a sufficiently good approximation must be searched by trying filters of different lengths and examining the outputs. Under this assumption, I tried several filter lengths for both algorithms, concluding that the optimal length for the MED filter was sixteen points, whereas it was five for the MEDD filter.

The MED algorithm became steady after the thirtieth iteration, reaching a Varimax value lower than that of the MEDD output (Table 1 and Figure 12a). This fact is clearly reflected in the resolution of the output. The recovered wavelet (Figure 6d,

top) and the delta function obtained by convolving f_D with the source wavelet (Figure 13) show that the filter f_D is a good inverse.

Example 2.—I chose as source signal the Ricker wavelet (forty units long), considered in the geophysical literature as a good estimation of the source signal in problems related to seismic prospecting. Analytically, it represents the second derivative of the Gaussian density (Robinson and Treitel, 1980). I considered two two-impulse traces. The second spike in the second trace shows a modification in spacing, polarity, and amplitude as compared with the first trace.

In this case, because of the particular characteristics of the source wavelet, the lengths of the filters had to be increased to 40 points in both methods.

Convergence of MED became steady after the ninth iteration. The Varimax norm of the MEDD output more than doubled the value of the MED output. The MED output exhibits a high percentage of noise, and as could be expected, its polarity was reversed (Figure 7).

On the other hand, the MEDD output is a very good approximation to the spike series: amplitude, polarity, and spacing have been preserved. The inversion of the f_D filter produces a highly satisfactory wavelet.

It can be confirmed through Figure 13 that f_D is quite a good approximation to the inverse of the true wavelet.

Example 3.—This example proposes a particularly severe deconvolution problem. The source wavelet is a complicated nonminimum phase wavelet 60 points long. Three two- to three-impulse randomly generated spike series were picked for this example.

The best outputs were obtained with filter lengths close to 60 points in both cases.

The Varimax values for both outputs are quite similar, that of the MEDD output being slightly higher. Convergence of the MED process became steady after the twelfth iteration. Polarity was reversed in both cases, and a considerable level of deconvolution noise can be observed in both outputs. Notwithstanding, the MEDD output shows an improved recovery of amplitudes and spacing (Figure 8).

The wavelet recovered by inversion of the f_D filter adjusts strikingly to the shape of the true wavelet, taking into account the reversal of polarity.

Figure 13 shows, in spite of noise, that the narrowness of the delta function ensures that f_D is a good approximation to the inverse of the source wavelet. As in example 2, a delay can be observed in the position of the reversed delta.

Table 1. Comparative values of Varimax and D norms for outputs obtained through filters resulting from MED and MEDD processing.

	Number of traces	Varimax norm		D norm	
		MED output	MEDD output	MED output	MEDD output
Example 1	1	0.3535	0.3600	0.6532	0.6631
Example 2	10	1.6065	2.1078	0.2217	0.2356
Example 3	2	0.5763	1.1960	0.6069	0.7317
Example 4	2	0.6080	0.6498	0.4758	0.5106
Example 5	3	0.7992	0.8132	0.4609	0.5758

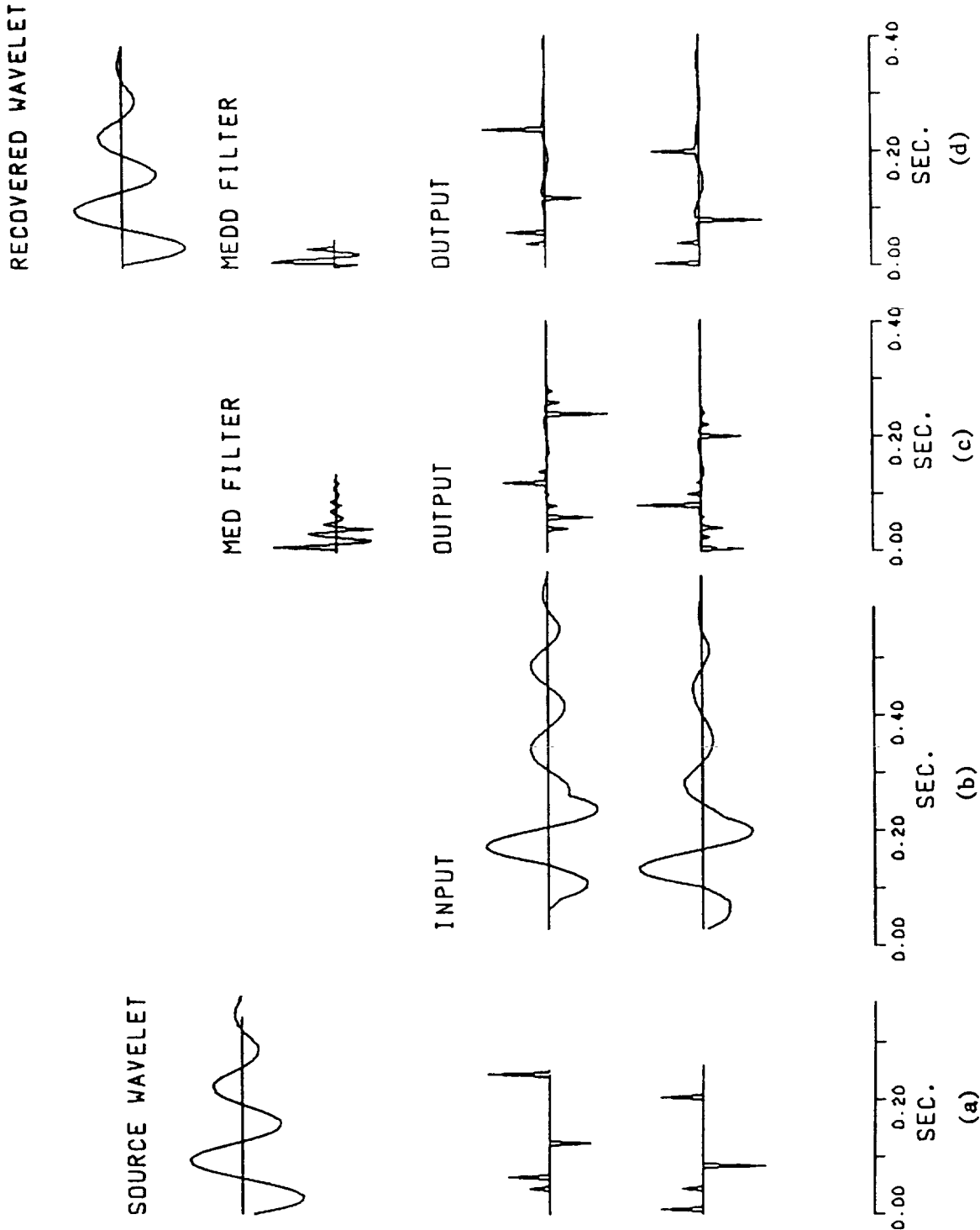


FIG. 6. Example 1. (a) Damped-down source wavelet and spike traces. (b) Input traces, no noise. (c) Output traces and filter obtained with the MED processing after fifty iterations. (d) Output traces, filter and recovered wavelet resulting from the MEDD processing.

RECOVERED WAVELET



SOURCE WAVELET



MEDD FILTER



MED FILTER



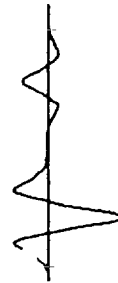
OUTPUT



OUTPUT



INPUT



(a)

(b)

(c)

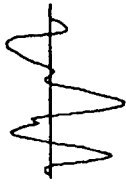
(d)

FIG. 7. Example 2. (a) Ricker wavelet and spike traces. (b) Input traces, no noise. (c) Output traces and filter resulting from the MED processing after 50 iterations. (d) Output traces, filter, and recovered wavelet obtained from the MEDD processing.

RECOVERED WAVELET



SOURCE WAVELET



MEDD FILTER



MED FILTER



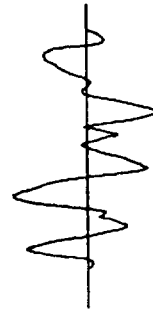
OUTPUT



OUTPUT



INPUT



(a)

(b)

(c)

(d)

FIG. 8. Example 3. (a) Nonminimum phase wavelet and random spike series. (b) Input traces, no noise. (c) Output traces and filter resulting from the MED processing after twenty iterations. (d) Output traces, filter, and recovered wavelet resulting from the MEDD processing.

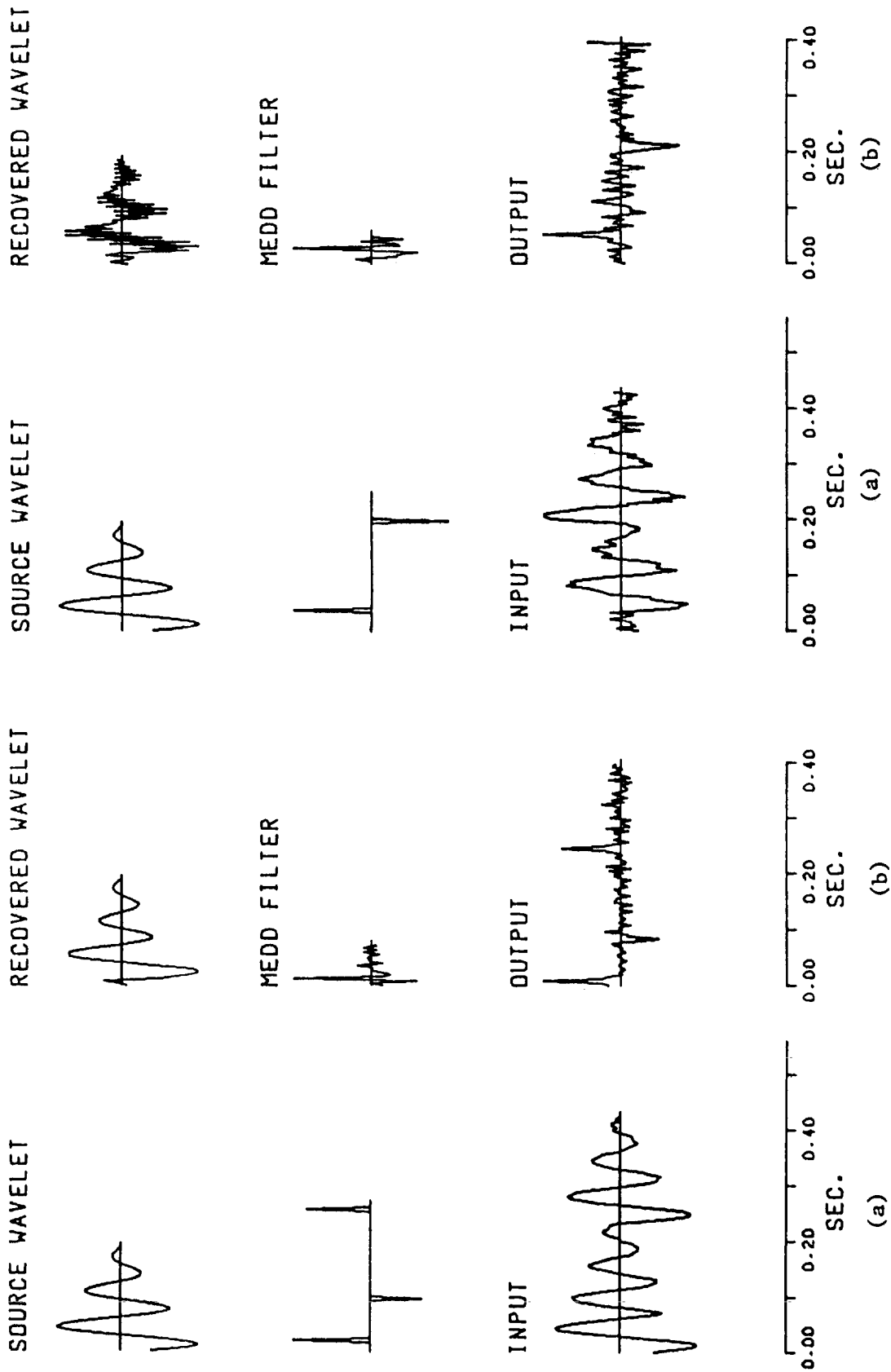


FIG. 9. Example 4. (a) Damped-down source wavelet, spike series and single trace input plus 5 percent white noise. (b) MEDD output, filter, and recovered wavelet.

FIG. 10. Example 5. (a) Damped-down source wavelet, spike series, and single trace input plus 25 percent white noise. (b) MEDD output, filter, and recovered wavelet.

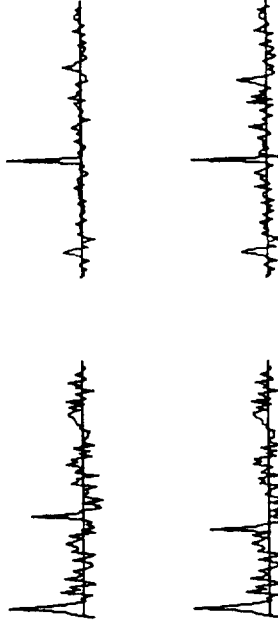
RECOVERED WAVELET RECOVERED WAVELET



MEDD FILTER



OUTPUT



SOURCE WAVELET



INPUT

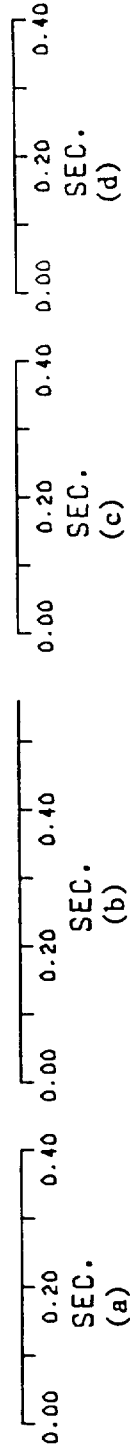
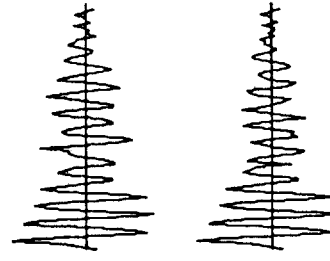


FIG. 11. Example 6. (a) Source wavelet and spike series. (b) Two trace input plus 15 percent white noise. (c) MEDD output and recovered wavelet for a five point long filter. (d) MEDD output and recovered wavelet for a 45 point long filter.

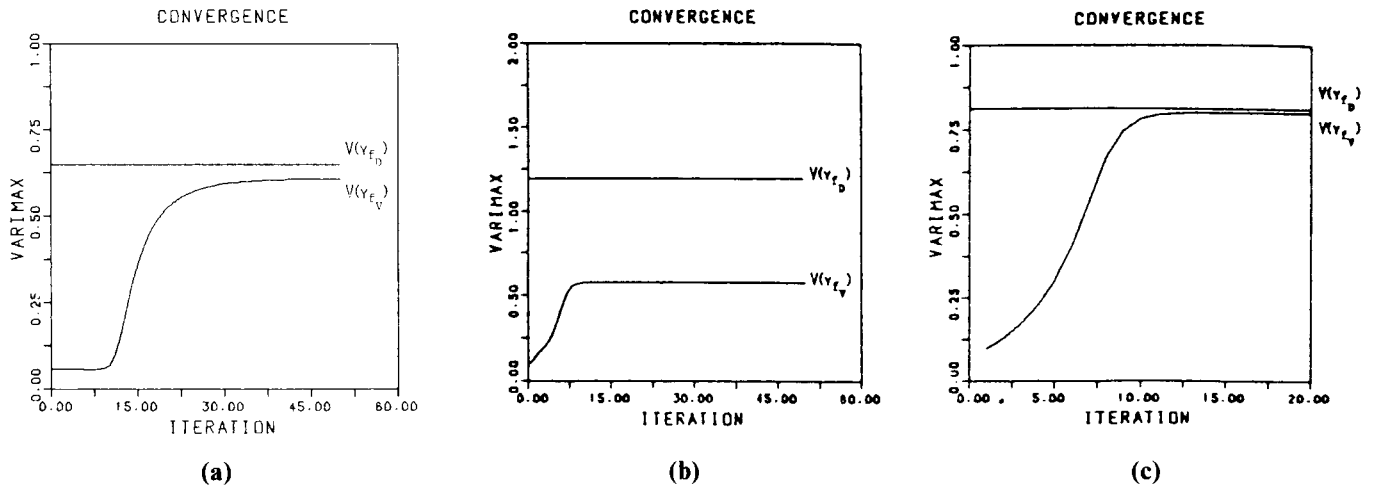


FIG. 12. Convergence of the MED process using the Varimax norm as compared with the V norm of the MEDD output (a) in example 1, (b) in example 2, and (c) in example 3.

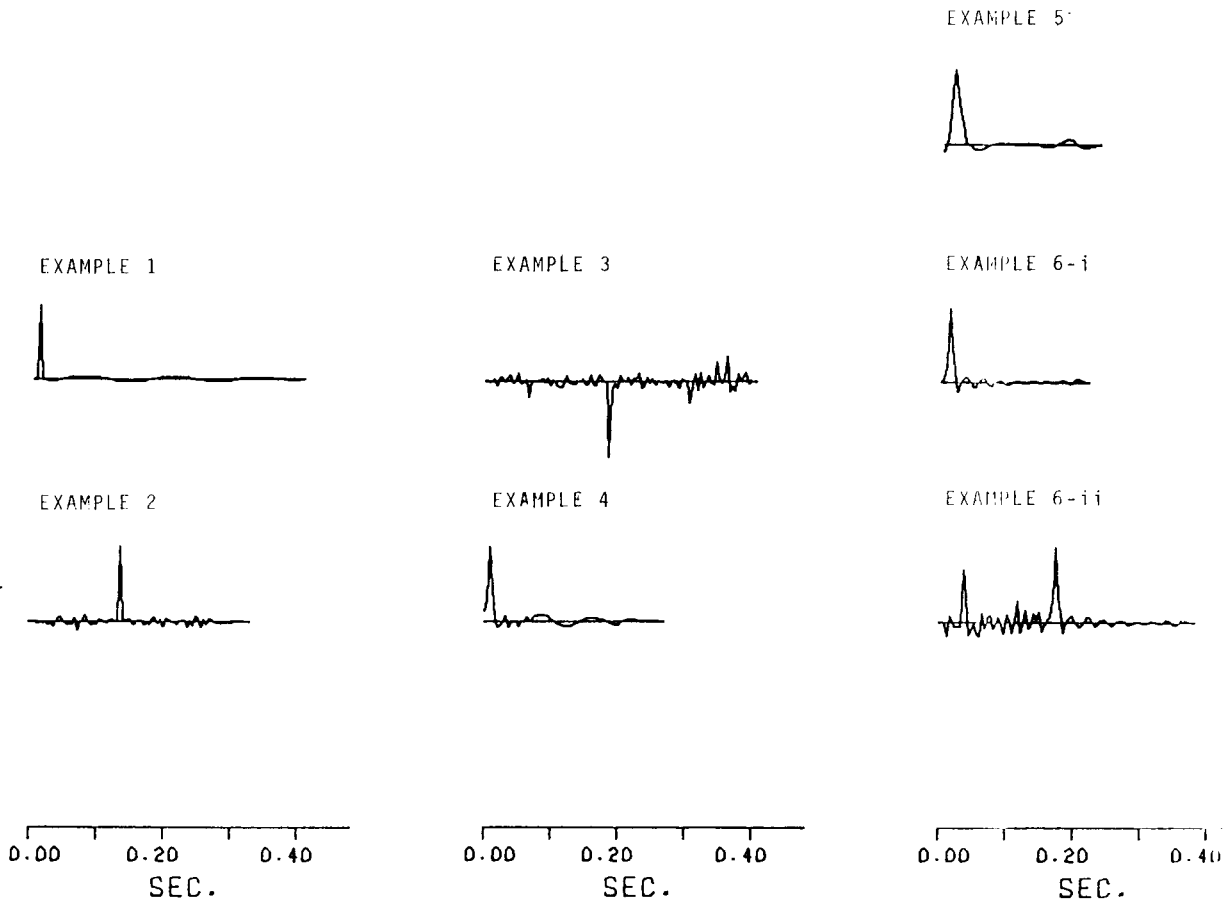


FIG. 13. Approximations to the delta function resulting from the convolution of the MEDD filters f_D with the corresponding source wavelets.

Examples 4 to 6. Model $x(t) = w(t) * q(t) + n(t)$

The aim is to study the stability of the MEDD algorithm when additive noise contaminates the data.

Examples 4 and 5.—The same source signal (50 units long) as in example 1 is used in these two examples. In both cases I took a single trace input plus 5 percent white noise (example 4) and 25 percent white noise (example 5).

Tests show that when white noise is added to the input, reduction in the length of the filter produces a better amplitude recovery of the impulses, but it also produces an increment in the amplitude of noise. Longer filters reduce remarkably the percentage of noise, but they can alter the amplitude of impulses even to the point of making them undistinguishable. This is a very important factor when deciding the length of the filter. This is discussed further in example 6.

The optimal filter lengths, in this sense, consisted of twenty points (example 4) and ten points in (example 5).

In example 4, the impulses of the output are perfectly distinguishable, even if the amplitude of the second spike is slightly diminished. In example 5, the output shows a high percentage of noise but the spikes preserve their amplitude (Figures 9 and 10).

A very good approximation of the true wavelet can be obtained in example 4 by inversion of the f_D filter; whereas in example 5 even if the recovered wavelet is contaminated with noise, it maintains the shape of the true wavelet (Figure 10, top right).

Example 6.—The damped source wavelet of this last example is a combination of sines of various frequencies, whose coefficients were taken randomly. It was discretized in 50 points. Two two-impulse series were chosen. Here the corresponding spikes of both traces had the same amplitude, but they were spaced differently. The input traces were contaminated with 15 percent white noise.

I studied the outputs produced by steadily varying the length of the filter. For lengths less than five points, the filter was not able to resolve the output impulses. For lengths larger than 60 points, the amplitude of the second impulses decreased to the point of being imperceptible. Figure 11 shows the MEDD outputs for a filter five points long (Figure 11c, example 6-i) and for a filter 45 points long (Figure 11d, example 6-ii).

The resolution of the output is superior in the shorter filter. This is confirmed by the inversion of the filters, which give in the case of the shorter filter a better approximation to the source wavelet than the longer one.

Figure 13 shows the delta functions obtained by convolving the filters obtained in these three examples with their source wavelets. It can be observed that broader delta functions are obtained when noise contaminates the input data.

CONCLUSIONS

I have proposed a new simplicity criterion in minimum entropy deconvolution, the D norm. This norm was developed following a geometrical interpretation of the Varimax norm proposed by Wiggins (1978).

I also define a norm-equivalence criterion which is an advance in the problem of norm choice and may possibly be beneficial in future work.

The D norm yields a noniterative algorithm for the computation of the deconvolution filter, which requires the inversion of a single autocorrelation matrix whose order is the length of the filter. In the considered examples, the optimal length for the filter f_D was shorter than, or at least equal to, the optimal length for the filter f_V .

Numerical tests show higher simplicity in outputs of the MEDD algorithm. This alone is not necessarily a measure of success, but when the reflectivity is reproduced successfully, it suggests a better signal-to-noise ratio for the MEDD output, which is definitely desirable.

Finally, stability in the presence of additive noise, which is one of the outstanding characteristics of the MED process, is markedly enhanced by using the D criterion.

Conventional noise suppression and stabilization techniques (e.g., adding a constant to the autocorrelation matrix \mathbf{R} , or solving the normal equations using spectral decomposition of that matrix) can be easily incorporated into the MEDD algorithm, which increases its practicality.

ACKNOWLEDGMENTS

I am indebted to the Dept. of Special Studies, Yacimientos Petrolíferos Fiscales, Argentina, for their technical advise and bibliography; to Lic. Jorge A. Fiora, Instituto Nacional de Tecnología Industrial, Argentina, for his invaluable cooperation in the preparation of plottings; and to the authorities of the Comisión Nacional de Investigaciones Espaciales, Argentina, for permitting me the use of their computational equipment. My very special thanks to Prof. Miguel Herrera—lamentably deceased in January 1984—for his permanent stimuli and useful comments, and to Ing. Abel Burna, YPF, Argentina, who introduced these topics to me.

I wish to thank the anonymous reviewers for constructive comments and suggestions.

REFERENCES

- Carrol, J. B., 1953, An analytical solution for approximating simple structure in factor analysis: *Psychometrika*, **18**, 23–38.
- Clayton, R. W., and Ulrych, T. J., 1977, A restoration method for impulsive functions: *Inst. of Elect. and Electron. Eng. Trans. Inf. Th.*, **23**, 262–264.
- Harman, H. H., 1960, *Modern factor analysis*: Univ. Chicago Press.
- Lines, L. R., and Ulrych, T. J., 1977, The old and the new in seismic deconvolution and wavelet estimation: *Geophys. Prosp.*, **25**, 512–540.
- Oldenburg, D. W., Levy, S., and Whittall, K. P., 1981, Wavelet estimation and deconvolution: *Geophysics*, **46**, 1528–1542.
- Ooe, M., and Ulrych, T. J., 1979, Minimum entropy deconvolution with an exponential transformation: *Geophys. Prosp.*, **27**, 458–473.
- Robinson, E. A., and Treitel, S., 1980, *Geophysical signal analysis*: Prentice-Hall, Inc.
- Ulrych, T. J., and Walker, C., 1982, Analytic minimum entropy deconvolution: *Geophysics*, **47**, 1295–1302.
- Wiggins, R. A., 1978, Minimum entropy deconvolution: *Geoxpl.*, **16**, 21–35.

APPENDIX A

THE EQUATION $y = \sum_k f_k v_k$

Let $\mathbf{x} = (x_1, \dots, x_n)$ be a sample of length n . The convolution of \mathbf{x} with a filter \mathbf{f} of length ℓ can be written in matrix form as in equation (4):

$$\mathbf{y} = \mathbf{f} \cdot \mathbf{X},$$

where the rows of \mathbf{X} are the vectors

$$\mathbf{v}_k = (\underbrace{0, \dots, 0}_{k-1}, x_1, \dots, x_n, \underbrace{0, \dots, 0}_{\ell-k}) \quad k = 1, \dots, \ell.$$

I show that under the assumption of a nonzero sample, the set of vectors $\{\mathbf{v}_1, \mathbf{v}_2, \dots, \mathbf{v}_\ell\}$ is linearly independent.

Following the hypothesis presented above there is a non-empty subset of $\{1, \dots, n\}$ formed by index i such that $x_i \neq 0$. Let v be the smallest index in the subset.

Now consider the submatrix \mathbf{X}' of \mathbf{X} formed by all the columns containing the entry x_v .

$$\begin{bmatrix} x_1 & x_2 & \cdots & \cdots & x_v & \cdots & \cdots & x_n & \cdots & 0 \\ \vdots & \vdots & \vdots & \vdots & \vdots & \vdots & \vdots & \vdots & \vdots & \vdots \\ 0 & \cdots & x_1 & x_2 & \cdots & \cdots & x_v & \cdots & \cdots & x_n \end{bmatrix}$$

\mathbf{X}'

This submatrix \mathbf{X}' is an upper triangular matrix since $x_i = 0$ for $i \in \{1, \dots, v-1\}$. Hence

$$\text{Det}(\mathbf{X}') = (x_v)^\ell \neq 0,$$

which means that

$$\text{rank}(\mathbf{X}') = \ell.$$

Therefore, column rank $(\mathbf{X}) \geq \ell$. But

$$\ell \geq \text{row rank}(\mathbf{X}) = \text{column rank}(\mathbf{X}) \geq \ell,$$

so that

$$\text{rank}(\mathbf{X}) = \ell$$

which implies that the set $\{\mathbf{v}_1, \dots, \mathbf{v}_\ell\}$ is linearly independent and spans a linear subspace W of \mathbb{R}^m of dimension ℓ .

APPENDIX B

THE D NORM AND THE SPIKING FILTER

This appendix shows a relation between the D norm defined in the case of a single sample and the spiking filter, the traditional method for the inversion of a wavelet (Robinson and Treitel, 1980).

In the spiking filter process, the norm

$$\|\mathbf{y} - \mathbf{e}_i\|^2$$

is minimized, for each $i = 1, \dots, m$, over the set of filters \mathbf{f} of length ℓ , where m is the length of the output

$$\mathbf{y} = \mathbf{x} * \mathbf{f}.$$

I already showed that the D norm is equivalent to minimizing

$$\|(\mathbf{y}/\|\mathbf{y}\|) - \mathbf{e}_i\|^2$$

for each $i = 1, \dots, m$. This means that both criteria differ only in the homogeneity factor $\|\mathbf{y}\|$. I prove that this difference is not a factor in the choice of the filter.

Let W be the linear subspace considered in Appendix A. The vector $\mathbf{w} \in W$ which minimizes $\|\mathbf{w} - \mathbf{e}_i\|$ is the orthogonal projection of \mathbf{e}_i over W . Assume that $\mathbf{e}_i \perp W$, which means that $\|\mathbf{w}\| \neq 0$. Therefore $(\mathbf{e}_i - \mathbf{w}) \perp W$.

Here I show that $\mathbf{w}_0 = \mathbf{w}/\|\mathbf{w}\|$ minimizes $\|(\mathbf{y}/\|\mathbf{y}\|) - \mathbf{e}_i\|^2$. Let \mathbf{y} be any nonzero vector of W , and take $\mathbf{y}_0 = \mathbf{y}/\|\mathbf{y}\|$. Then

$$1 = \|\mathbf{y}_0\| \leq \|\mathbf{y}_0 - \mathbf{w}\| + \|\mathbf{w}\|$$

and

$$1 = \|\mathbf{w}_0\| = \|\mathbf{w}_0 - \mathbf{w}\| + \|\mathbf{w}\|$$

since $\mathbf{w} = \|\mathbf{w}\|\mathbf{w}_0$ and $\|\mathbf{w}\| \leq 1$. This means that

$$\|\mathbf{w}_0 - \mathbf{w}\| \leq \|\mathbf{y}_0 - \mathbf{w}\|.$$

Hence

$$\|\mathbf{w}_0 - \mathbf{w}\|^2 \leq \|\mathbf{y}_0 - \mathbf{w}\|^2.$$

Then

$$\begin{aligned} \|\mathbf{w}_0 - \mathbf{e}_i\|^2 &= \|\mathbf{w}_0 - \mathbf{w}\|^2 + \|\mathbf{w} - \mathbf{e}_i\|^2 \\ &\leq \|\mathbf{y}_0 - \mathbf{w}\|^2 + \|\mathbf{w} - \mathbf{e}_i\|^2 \\ &= \|\mathbf{y}_0 - \mathbf{e}_i\|^2. \end{aligned}$$

This clearly shows that \mathbf{w} minimizes $\|(\mathbf{y}/\|\mathbf{y}\|) - \mathbf{e}_i\|^2$.

APPENDIX C

DIFFERENCES BETWEEN THE D NORM AND THE V NORM

In order to maximize the D norm, it is necessary to compute

$$\max_f |y_i|/\|y\|. \quad (C-1)$$

Clearly, maximization of $|y_i|/\|y\|$ is equivalent to maximization of its square $y_i^2/\|y\|^2$.

Denote $y^2 = (y_1^2, \dots, y_m^2)$. Hence, $\|y\|^{-2}y^2$ belongs to the set H previously defined. It is then clear that maximization (C-1) is equivalent to minimization of the distance from $\|y\|^{-2}y^2$ to the vertex e_i in H .

On the other hand, I have shown that the Varimax norm is equivalent to maximizing the distance from $\|y\|^{-2}y^2$ to the barycenter \mathbf{B} of H . Consequently, the behavior of norms V and D can be described as follows

- (a) For every filter \mathbf{f} , \mathbf{y} is obtained from $\mathbf{y} = \mathbf{f} * \mathbf{x}$.
- (b) Then \mathbf{y} is transformed by $\mathbf{y} \rightarrow \|y\|^{-2}y^2 \in H$
- (c) At this point the norms differ:

- (1) The D norm measures the distance from this point to the nearest vertex [i.e., $\min_k \|(\mathbf{y}^2/\|y\|^2) - \mathbf{e}_k\|$].
- (2) The V norm measures the distance from this point to the barycenter \mathbf{B} of H . [i.e., $\|(\mathbf{y}^2/\|y\|^2) - \mathbf{B}\|$].

In Figure C-1 this situation is shown for $m = 3$.

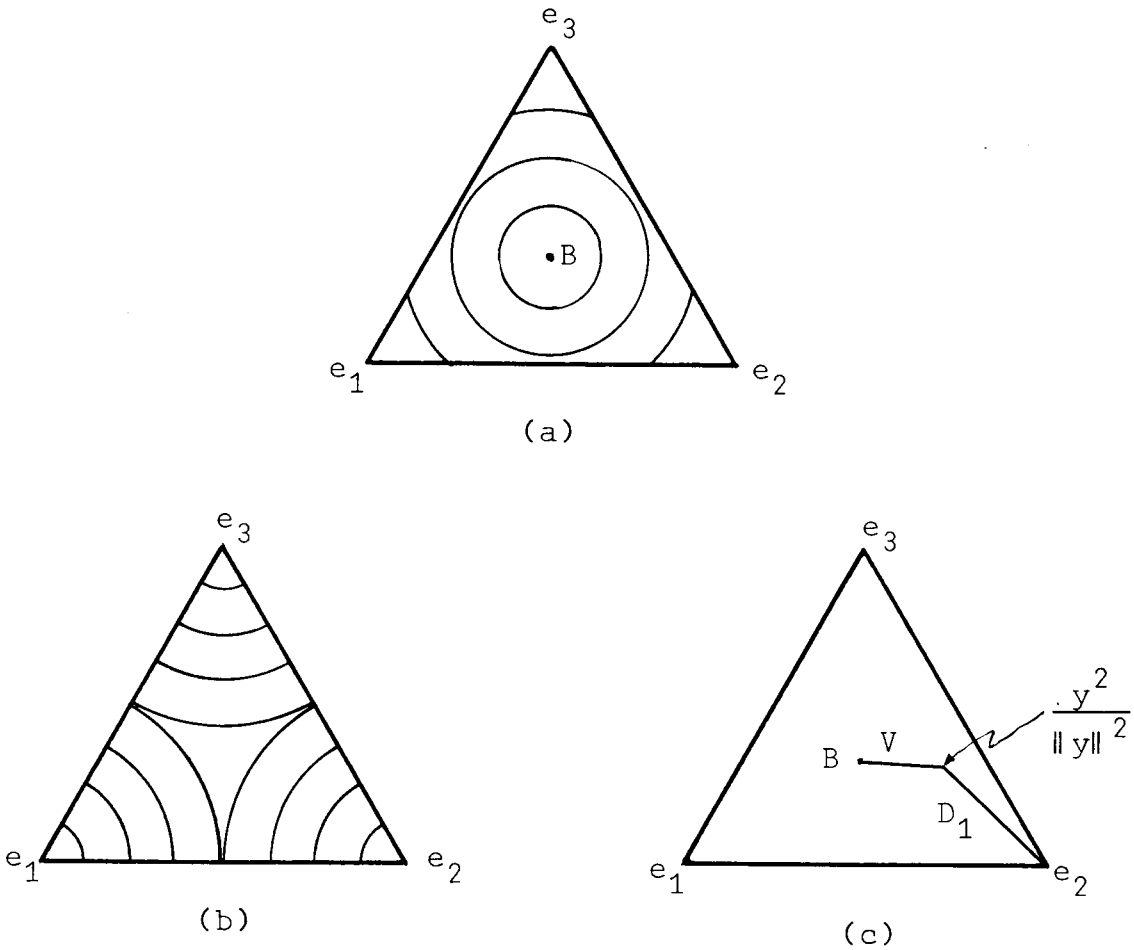
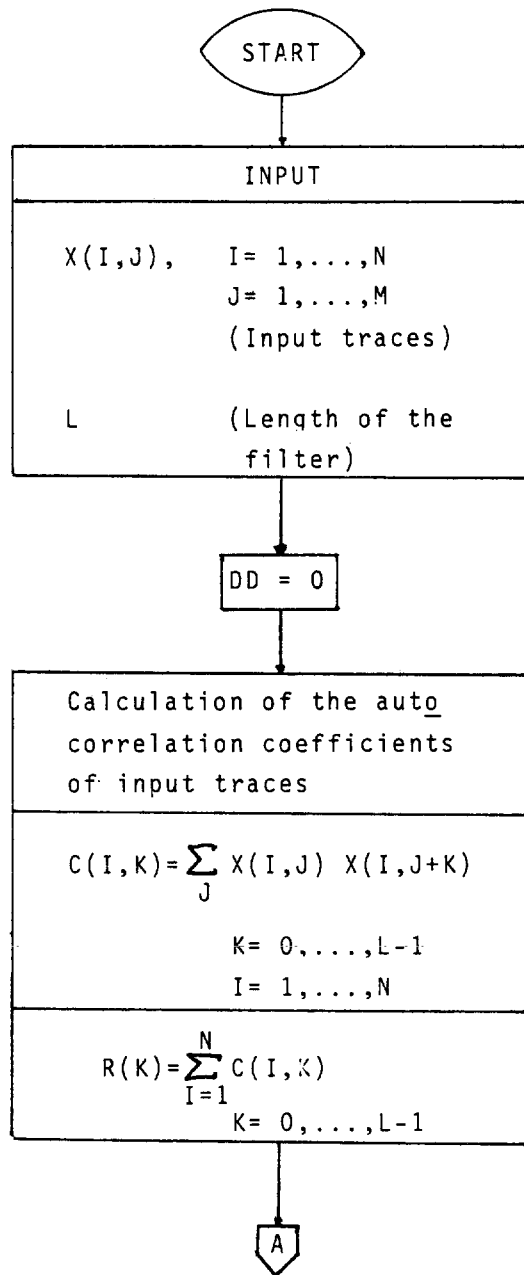
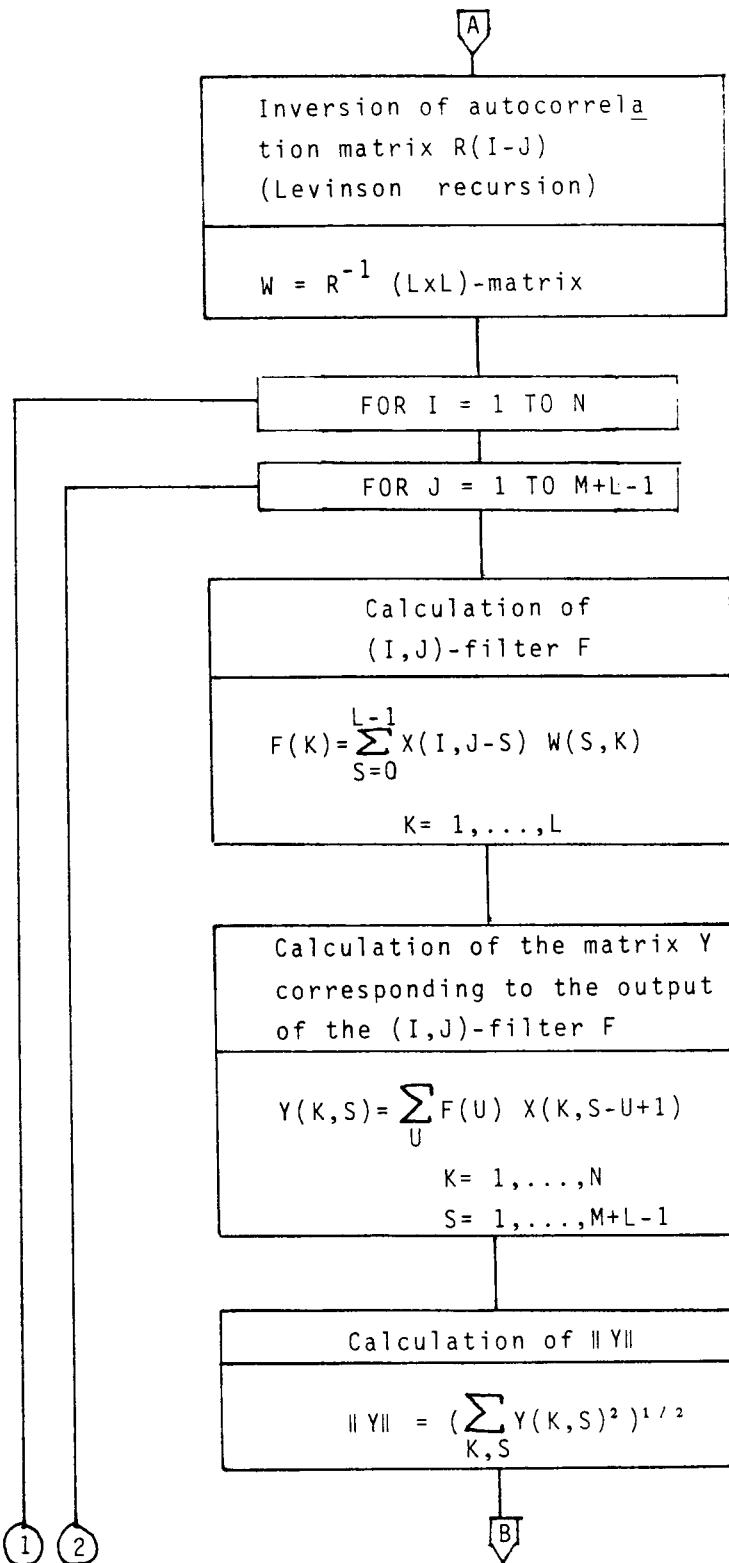


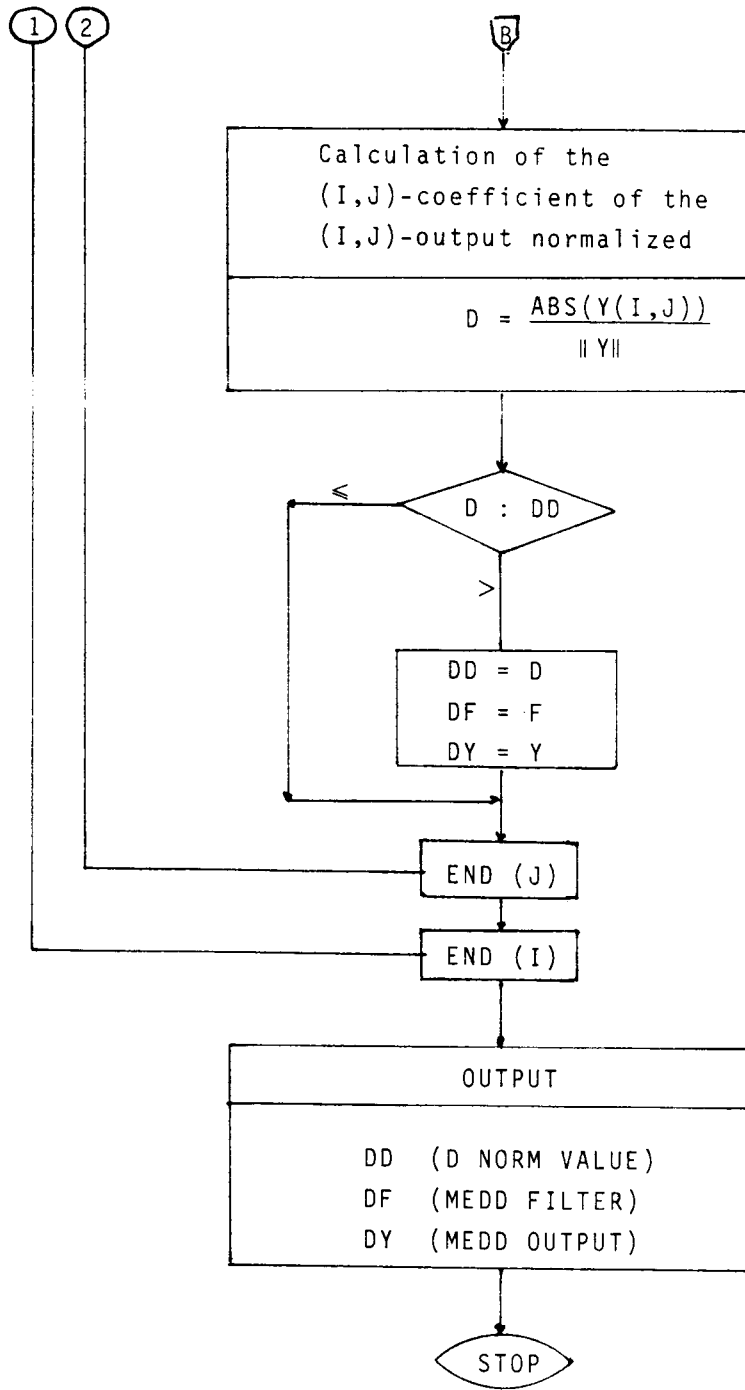
FIG. C-1. Contour lines for (a) V norm and (b) D norm. (c) V and D norms of a vector $y^2/\|y\|^2$.

APPENDIX D

FLOW CHART OF THE MEDD ALGORITHM







NOTE: We consider
 $X(H,S) = 0$ if $S \neq 1, \dots, M$